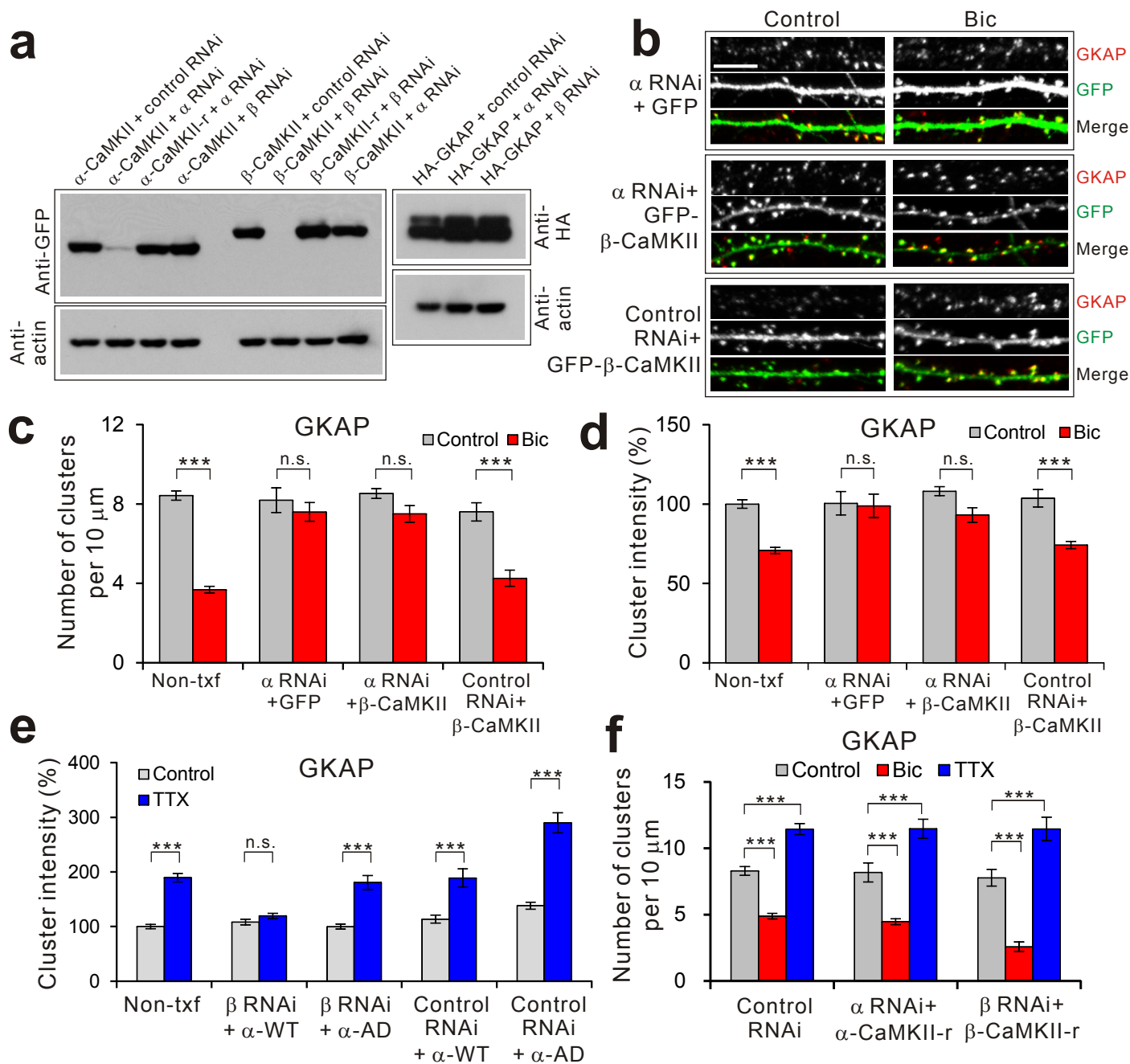
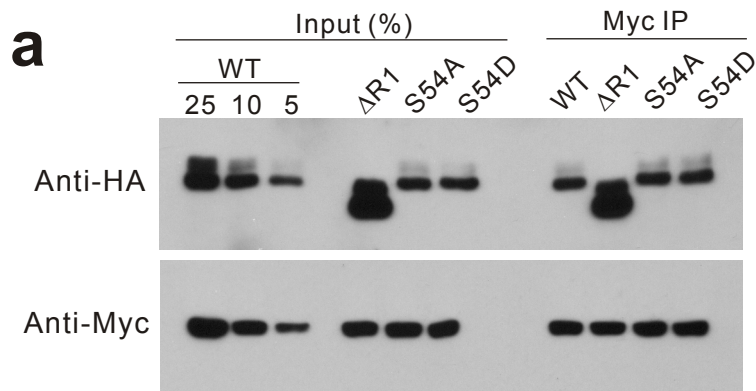


# GKAP/SAPAP orchestrates activity-dependent postsynaptic protein remodeling and homeostatic scaling

Seung Min Shin, Nanyan Zhang, Jonathan Hansen, Nashaat Z. Gerges, Daniel T.S. Pak, Morgan Sheng & Sang H. Lee



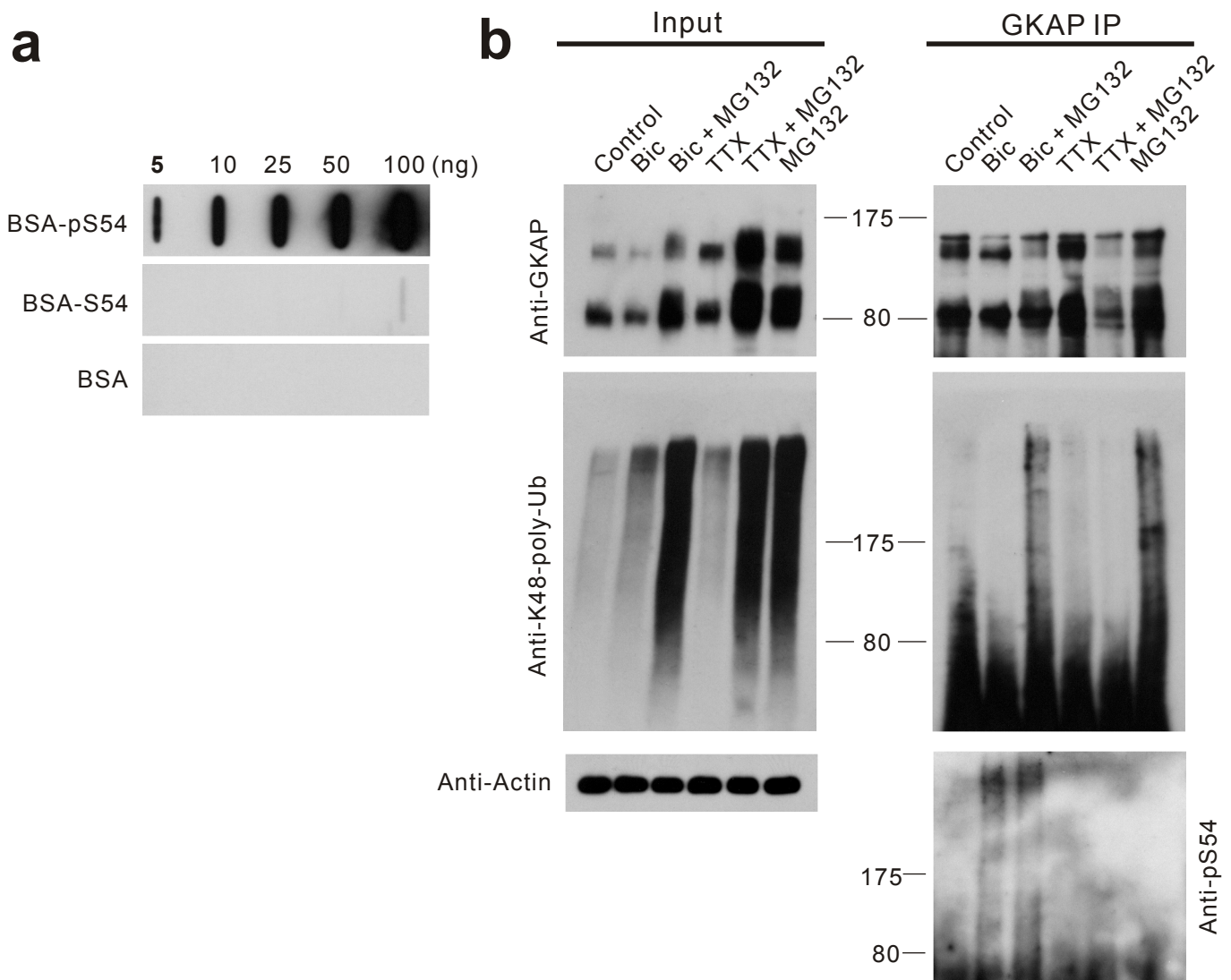
**Supplementary Figure 1** Effect of isoform-specific CaMKII RNAi on activity-dependent turnover of GKAP. (a) Specificity of  $\alpha$  and  $\beta$  RNAi. COS cells were transfected with GFP-tagged CaMKII isoforms and respective RNAi expression constructs as indicated above lanes and examined for protein levels.  $\alpha$ -CaMKII-r and  $\beta$ -CaMKII-r denote RNAi-resistant rescue constructs. Actin blot is shown as a loading control. (b-d)  $\beta$ -CaMKII overexpression cannot rescue  $\alpha$  RNAi that blocks Bic-induced removal of GKAP from synapses. Hippocampal neurons were transfected with constructs as indicated and examined for the changes in GKAP clusters (red) by immuno-fluorescence staining. (b) Representative images. Scale bar, 5  $\mu$ m. (c,d) Quantification of the effect of  $\beta$ -CaMKII and  $\alpha$  RNAi on GKAP turnover at synapses measured by cluster density (c) and intensity (d).  $n > 20$  per group. (e) Quantification of  $\beta$  RNAi rescue by  $\alpha$ -CaMKII-AD ( $\alpha$ -AD) measured by changes in the synaptic intensity of GKAP.  $n > 20$  per each construct. (f) Rescue of  $\alpha$  and  $\beta$  RNAi-induced defects of GKAP turnover by the co-expression of RNAi-resistant  $\alpha$ -CaMKII-r and  $\beta$ -CaMKII-r. \*\*\* $P < 0.001$ , n.s., not significant.



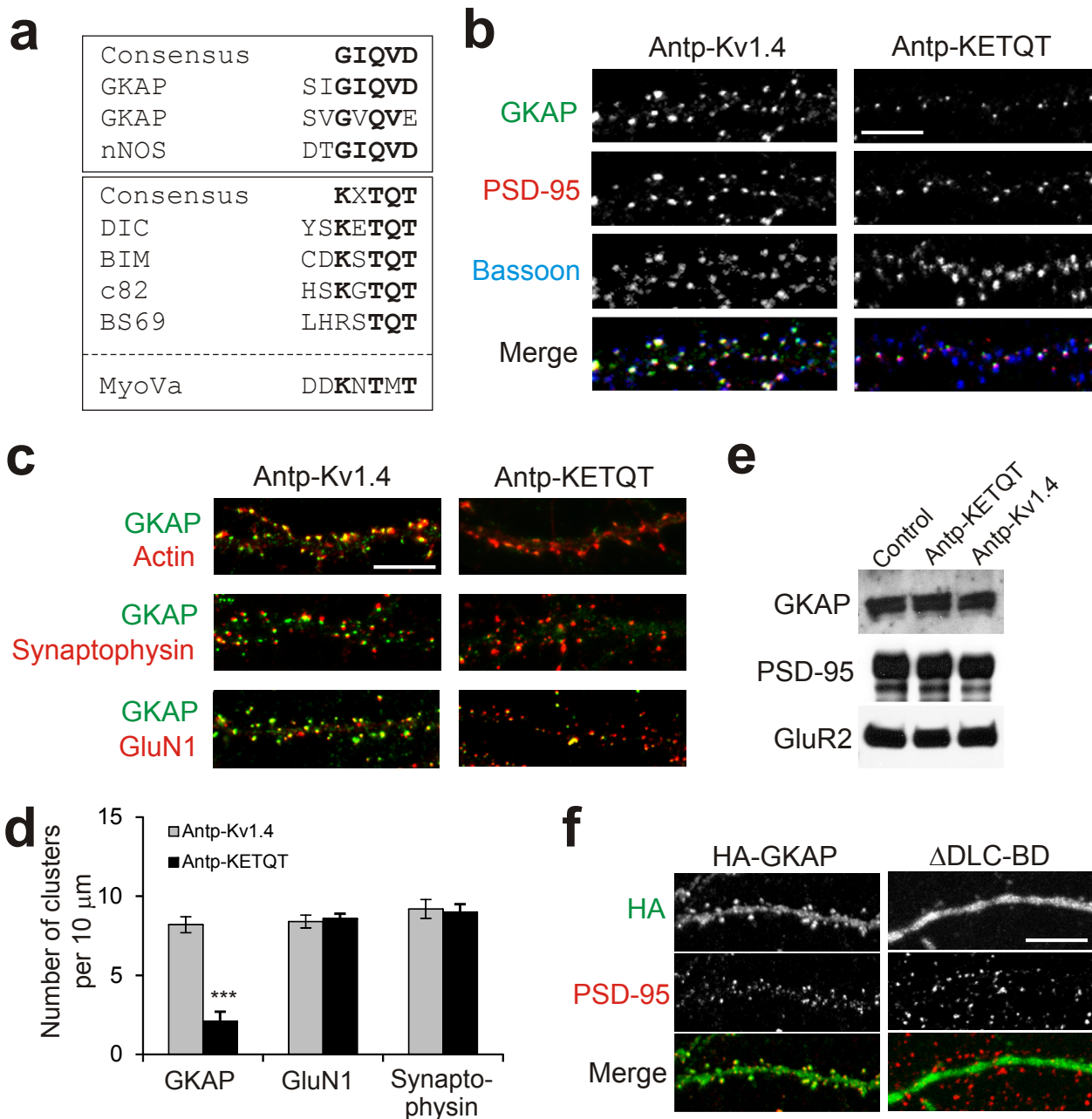
**b**

Bait	Mutation	Prey	
		PSD-95 GK	DLC2
R1R2 (aa 46-102)	WT	++++	N/A
	S54A	+	N/A
	S54D	+	N/A
	S83A	++++	N/A
	S83D	++++	N/A
	S54&S83A	+	N/A
	S54&S83D	+	N/A
R3R5 (aa 96-247)	WT	++++	N/A
	S114A	++++	N/A
	S114D	++++	N/A
	S148A	++++	N/A
	S148D	++++	N/A
	S201A	+	N/A
	S201D	+	N/A
Full-length GKAP	WT	++++	+++
	S54A	++++	+++
	S54D	++++	+++
	S83A	++++	+++
	S83D	++++	+++
	S54&S83A	++++	+++
	S54&S83D	++++	+++
	S114A	++++	+++
	S114D	++++	+++
	S148A	++++	+++
	S148D	++++	+++
	S201A	++++	+++
	S201D	++++	+++
	S54&S201A	+	+++
	S54&S201D	+	+++
$\Delta$ R1	++++	+++	

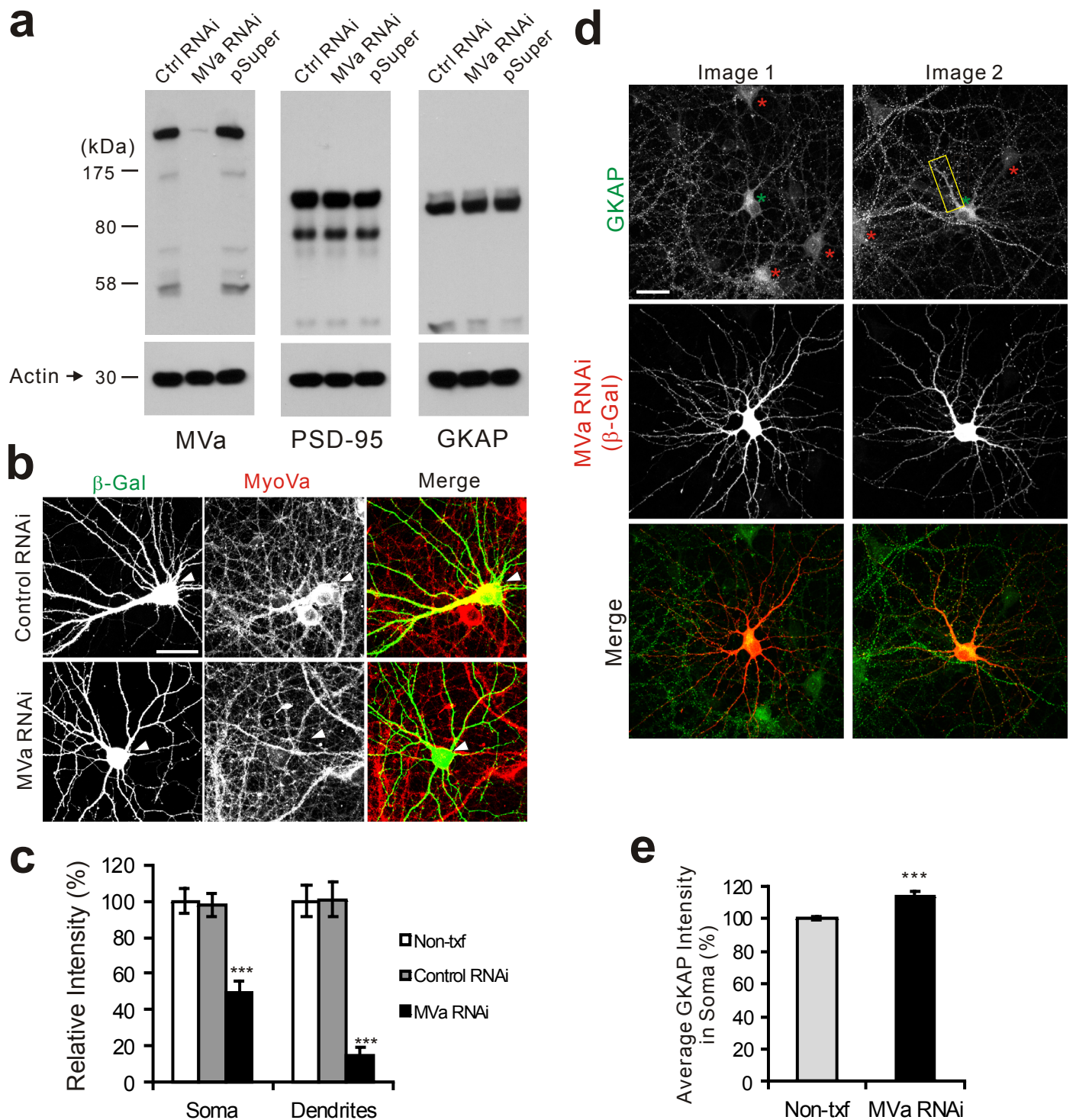
**Supplementary Figure 2** Effect of various mutations in GKAP on the interaction of GKAP with PSD-95 and DLC2. **(a)** Co-immunoprecipitation of PSD-95 with various GKAP mutants. HA-tagged GKAP WT,  $\Delta$ R1, S54A, or S54D were co-transfected with myc-PSD-95 into COS cells, immunoprecipitated with myc-agarose beads, and examined for co-immunoprecipitation by Western blotting. **(b)** Yeast two hybrid tests of WT and phospho-site mutant GKAP interaction with PSD-95 GK domain and DLC2. Interaction strength is determined by the time taken for yeast colonies turn to blue in X-gal filter assays at room temperature. +++++, < 15 min; +++, < 30 min; +, > 1.5 h. N/A, not analyzed.



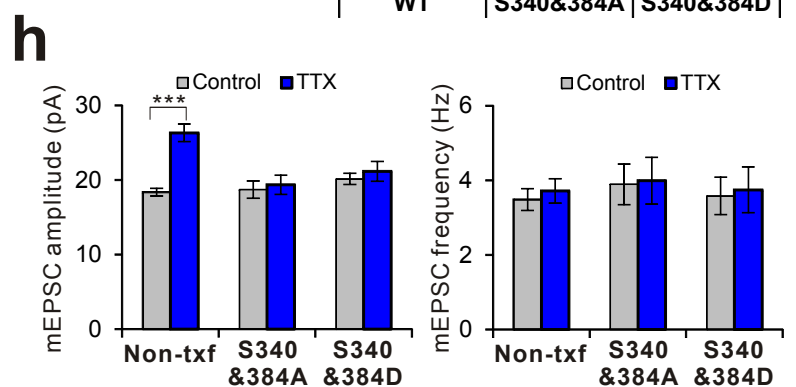
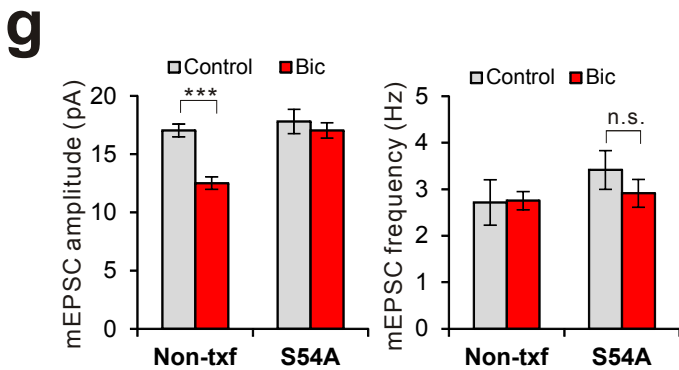
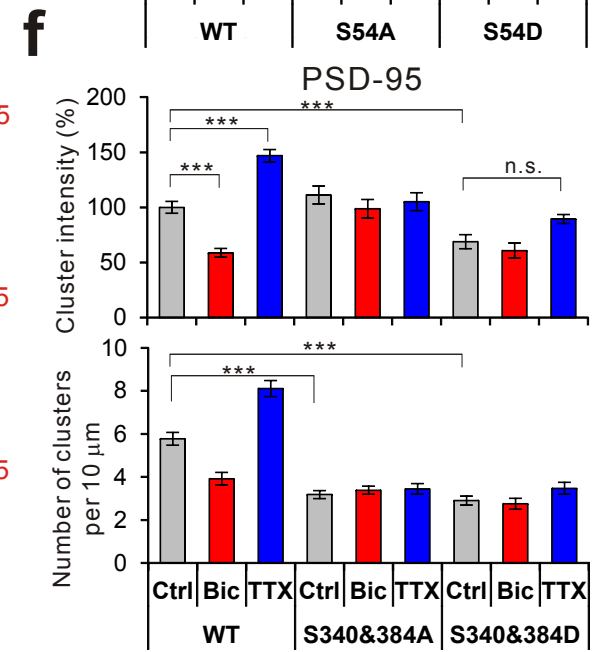
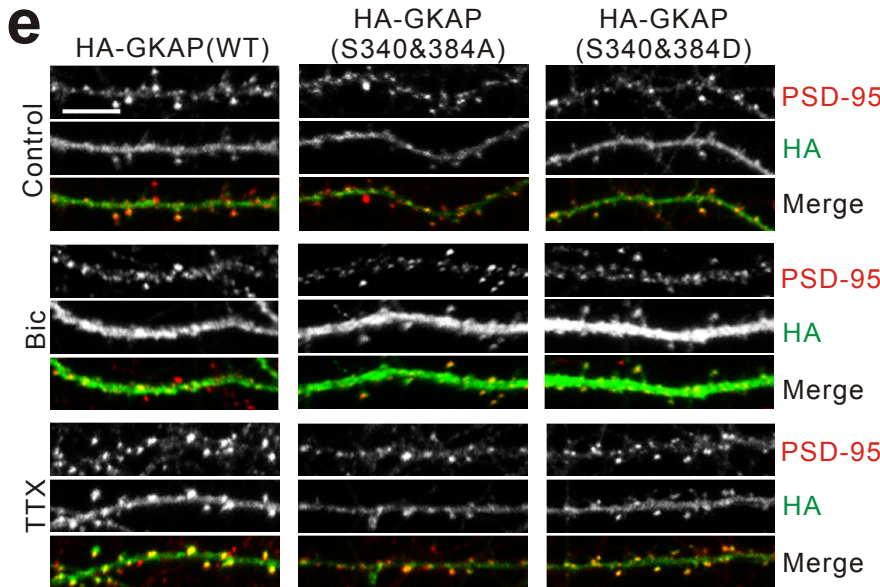
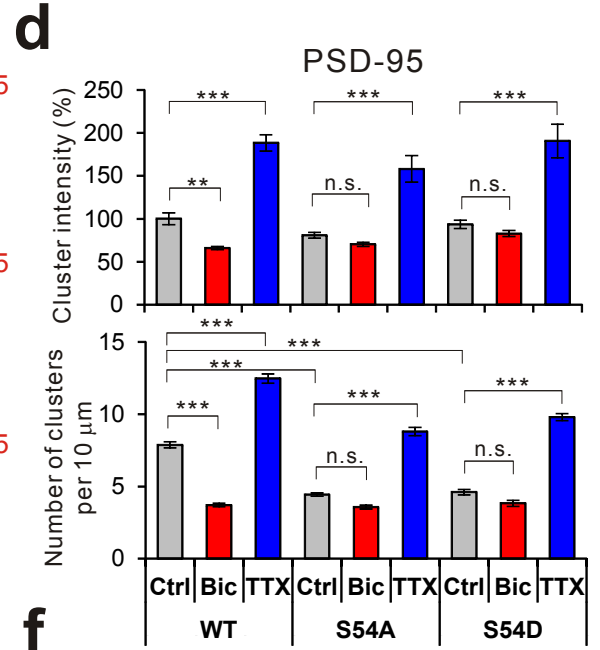
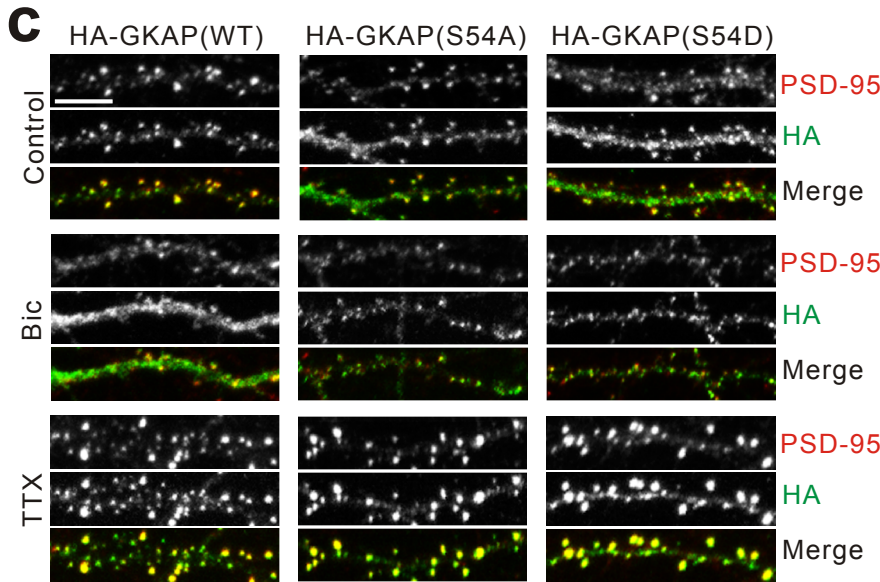
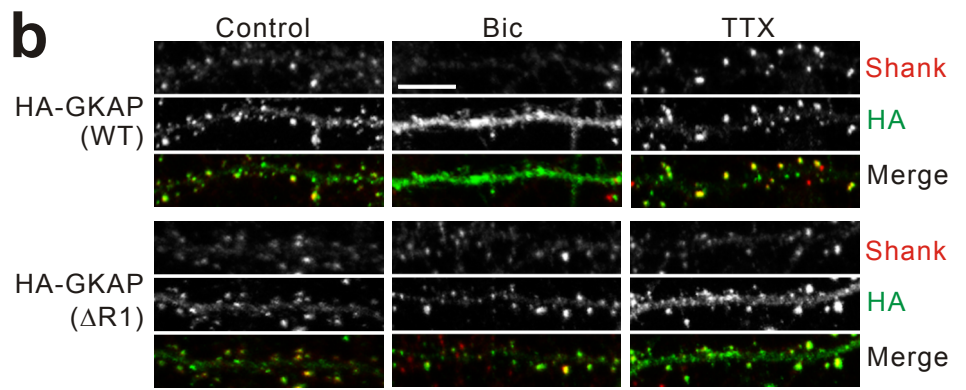
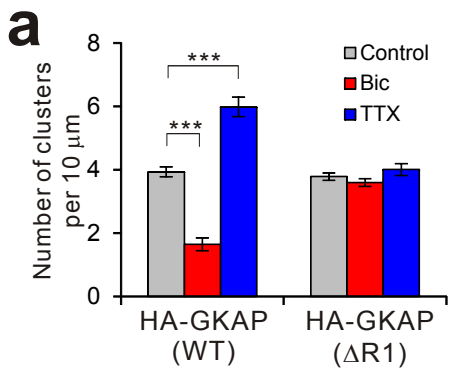
**Supplementary Figure 3** Activity-dependent phosphorylation of S54 and poly-ubiquitination of GKAP in hippocampal culture neurons. **(a)** Specificity of anti-pS54 antibody. Various amount of BSA, BSA conjugated pS54, or non-phosphorylated BSA conjugated WT peptide (as indicated above) were loaded onto PVDF membrane using a slot blotting apparatus and examined by Western blotting with anti-pS54 antibody. **(b)** S54 phosphorylation and poly-ubiquitination of immunoprecipitated GKAP. Hippocampal neurons (12 DIV, plated at 400 kcells/well in 6-well plate) were treated as indicated above lanes for 14 h and total lysates were immunoprecipitated with anti-GKAP antibody under denaturing conditions. Immunoprecipitates were examined for poly-ubiquitination (Anti-K48 poly-Ub antibody) and S54 phosphorylation (anti-pS54). Anti-actin antibody was used as loading control for the input. Duplicate experiments showed similar results.



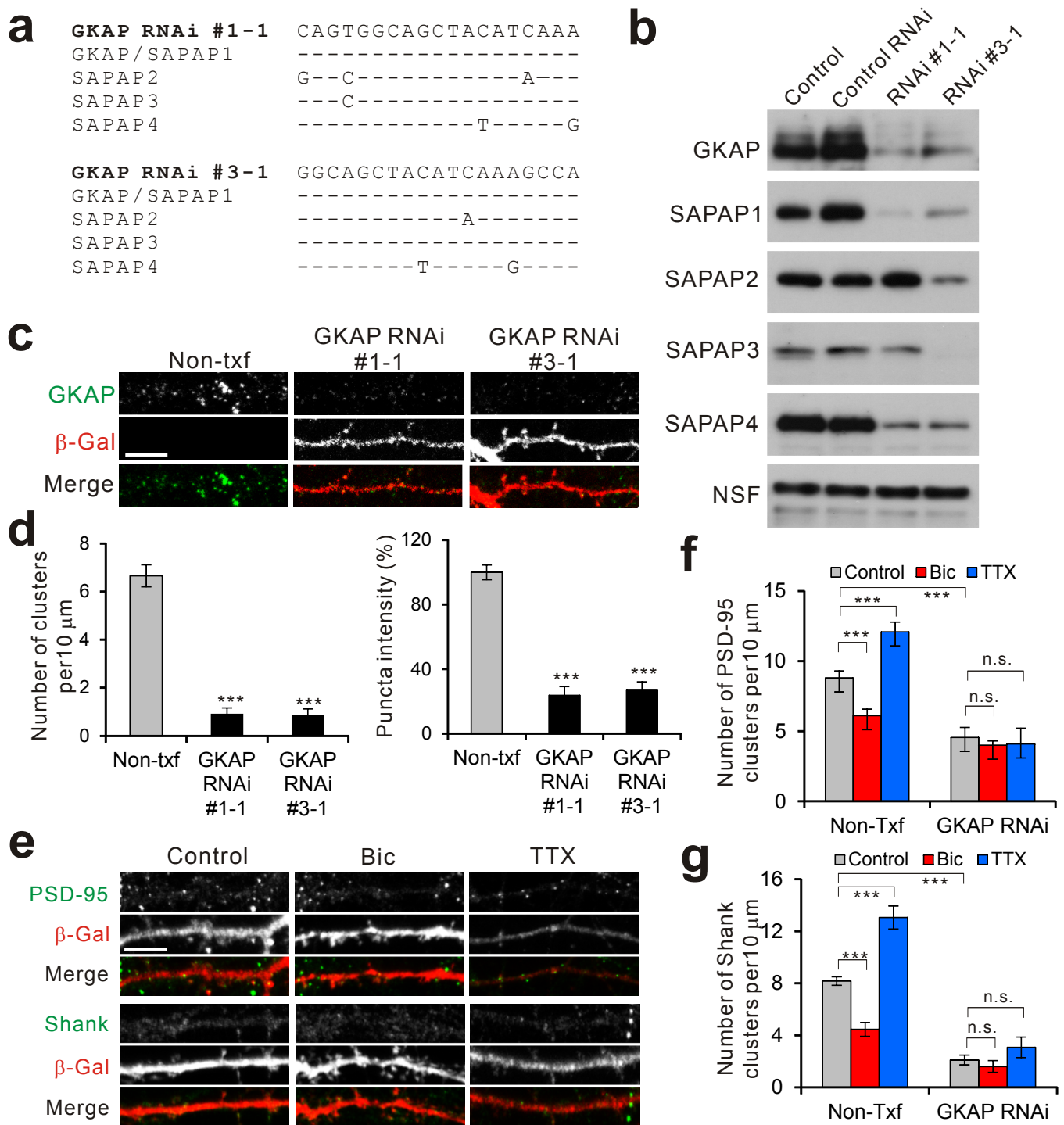
**Supplementary Figure 4** The role DLC interaction for synaptic targeting of GKAP. **(a)** Consensus amino acid sequence for DLC interaction. **(b)** Effect of Antp-Kv1.4 and Antp-KETQT peptide incubation (20  $\mu\text{M}$ , 18 h) in hippocampal neurons (16 DIV) on the synaptic clustering of GKAP, PSD-95, and Bassoon. **(c)** Effect of Antp-Kv1.4 and Antp-KETQT peptide on actin, synaptophysin, or GluN1 clusters, co-examined with GKAP (green). **(d)** Quantification of Antp-peptide effect on the cluster density of GKAP, GluN1, and synaptophysin.  $n = 20$  per condition. \*\*\* $P < 0.001$ . **(e)** Effect of Antp-peptides on the total protein levels of GKAP, PSD-95 and GluR2. **(f)** Defective synaptic targeting of HA-GKAP ( $\Delta\text{DLC-BD}$ ). Note that the HA staining for  $\Delta\text{DLC-BD}$  mutant is mostly limited within the dendritic shaft, while that of WT shows strong staining in the dendritic spines.



**Supplementary Figure 5** Specificity of MVa RNAi and its effect on GKAP (a) Specific and efficient knockdown of MVa by MVa RNAi in COS cells. MVa RNAi, control RNAi (Zn-T3) or empty pSUPER vector was co-transfected with either MVa, PSD-95, or GKAP in COS cells. Total lysates were examined for the protein levels of MVa, PSD-95 or GKAP. Actin blots are used as loading controls. (b) Effective knockdown of endogenous MVa in hippocampal neurons by MVa RNAi. Hippocampal neurons were transfected with either control RNAi or MVa RNAi and immunostained for MVa (red). Arrow heads show the specific reduction of MVa signal in the soma of MVa RNAi-transfected neurons (green). (c) Quantification of MVa RNAi effect measured by the MVa immunostaining intensity from the soma and dendrites.  $n=15$  per condition.  $***P < 0.001$ . (d) Representative images of neurons showing increased immunostaining intensity of GKAP in the soma (marked by \*) and dendritic shaft (yellow box) of MVa RNAi-transfected neurons, compared to non-transfected neighboring neurons (\*). (e) Quantification of average GKAP intensity in the soma of MVa-transfected and non-txf neurons.  $n = 23$ ,  $*** P < 0.001$ . Scale bars, 20  $\mu\text{m}$ .

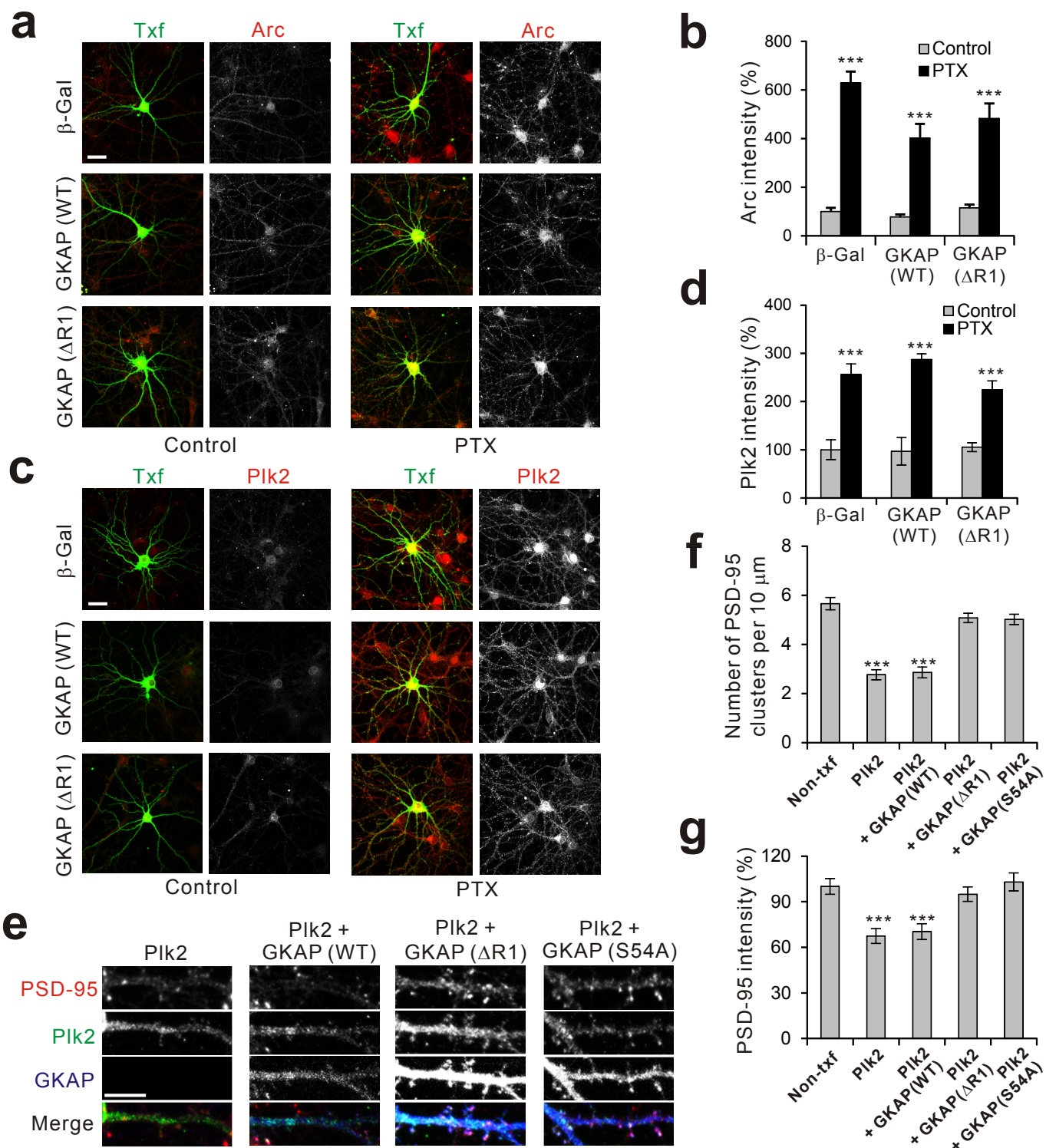


**Supplementary Figure 6** Effect of GKAP mutants on the activity-dependent turnover of endogenous PSD-95, Shank, and synaptic scaling. **(a)** Quantification of activity-dependent changes of transfected WT and  $\Delta R1$  HA-GKAP, measured by HA puncta density.  $n > 20$  per condition. **(b)** Representative images showing the effect of HA-GKAP (WT) and HA-GKAP ( $\Delta R1$ ) on the activity-dependent turnover of endogenous Shank. **(c)** Effect of HA-GKAP (S54A) or HA-GKAP (S54D) overexpression on the Bic- and TTX-dependent turnover of endogenous PSD-95. **(d)** Quantification of activity-dependent changes of endogenous PSD-95 in WT, S54A, and S54D-transfected neurons, measured by changes in cluster intensity (top) and cluster density (bottom).  $n > 30$  per condition.  $***P < 0.001$ ,  $**P < 0.01$ , n.s., not significant. **(e)** Effect of HA-GKAP S340&S384A or S340&384D overexpression on the activity-dependent turnover of endogenous PSD-95. **(f)** Quantification of activity-dependent changes of endogenous PSD-95 in S340&S384A or S340&384D transfected neurons.  $n > 30$  per condition.  $***P < 0.001$ , n.s., not significant. **(g)** HA-GKAP S54A overexpression blocks Bic-induced synaptic scaling.  $n > 10$  per condition.  $***P < 0.001$ , n.s., not significant. **(h)** HA-GKAP S340&384A and S340&384D mutants block TTX-induced synaptic scaling.  $n > 10$  per condition.  $***P < 0.001$ . Scale bars, 5  $\mu\text{m}$ .

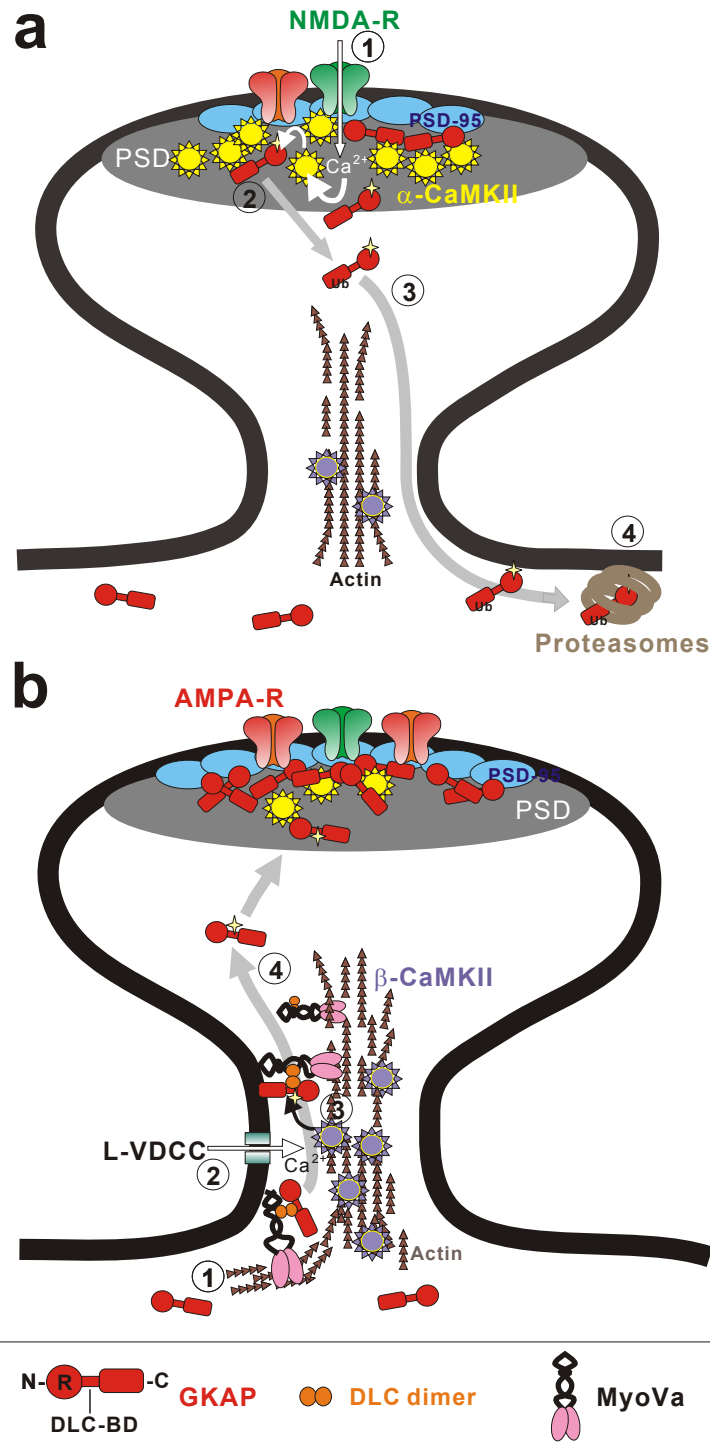


**Supplementary Figure 7** Specificity of GKAP RNAi and its effect on activity-dependent turnover of PSD-95 and Shank. **(a)** Design basis of GKAP RNAi. Nucleotide sequence alignment of rat GKAP/SAPAP cDNAs in the GKAP RNAi targeting regions. **(b)** Effective and specific knockdown of all 4 SAPAPs by GKAP RNAi #3-1. Various GKAPs or NSF (as indicated on the left; all myc-tagged) were transfected in COS cells either without (Control) or together with Control RNAi, GKAP RNAi #1-1, or #3-1. The effect of RNAi was examined by anti-myc blotting. **(c)** Effect of GKAP RNAi on endogenous GKAP/SAPAP.  $\beta$ -Gal was co-transfected as a transfection marker. **(d)** Quantification of GKAP RNAi on endogenous GKAP puncta density (left) and intensity (right).  $n > 12$  per condition. **(e-g)** GKAP RNAi (#3-1) blocks activity-dependent turnover of PSD-95 and Shank. Representative images are shown in **(e)** and quantified in **(f,g)**.  $n > 12$  per condition. \*\*\* $P < 0.001$ , n.s., not significant. Scale bars, 5  $\mu\text{m}$ .

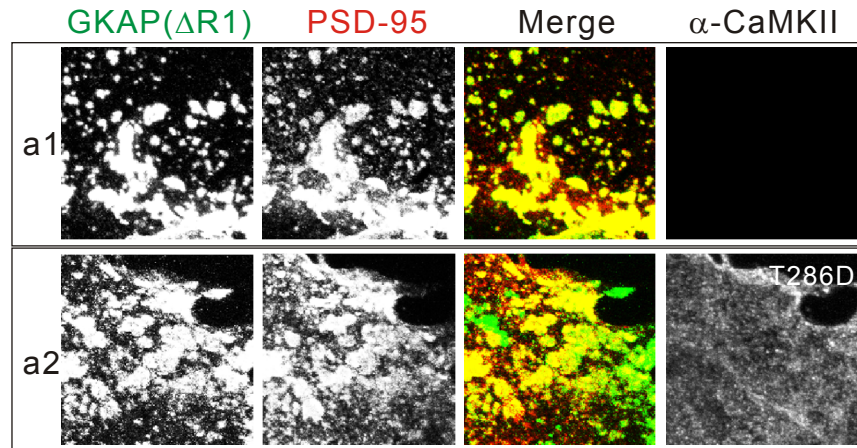




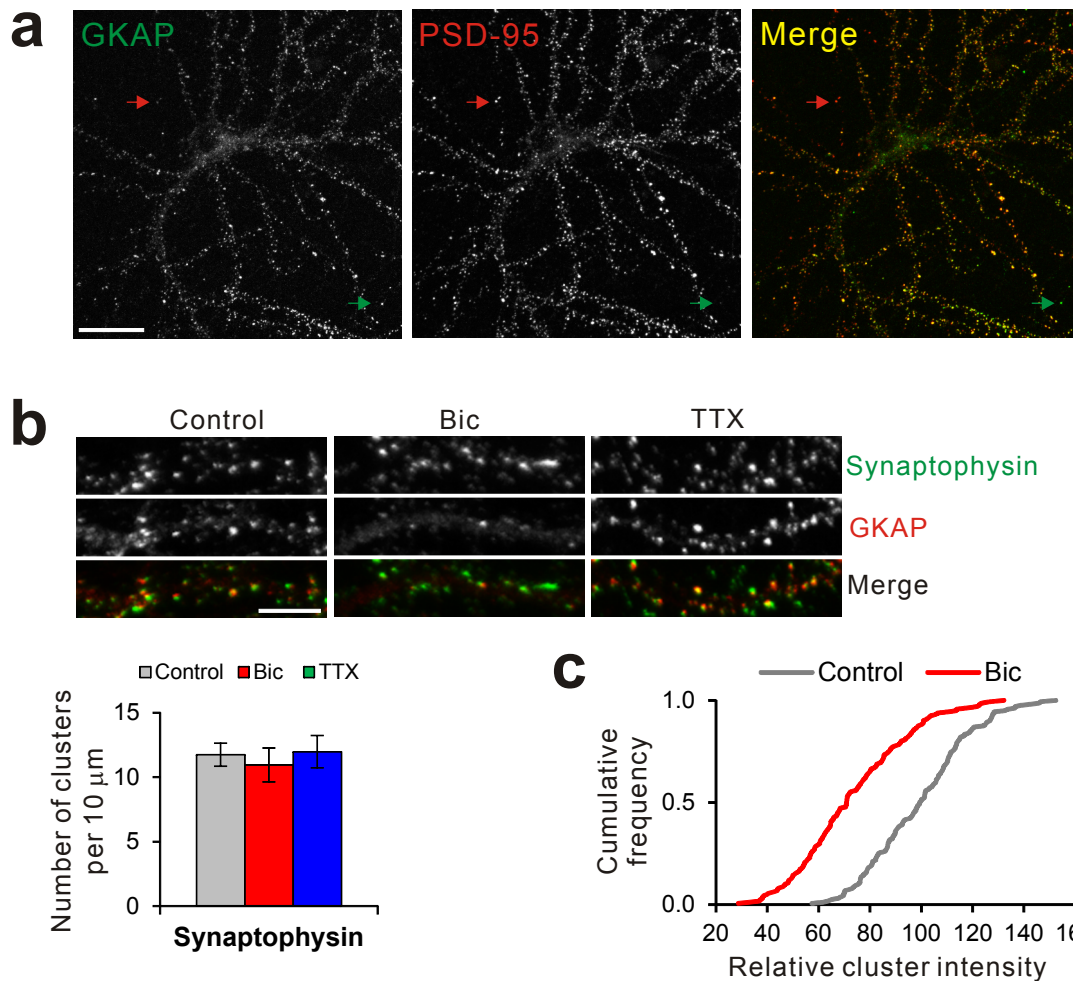
**Supplementary Figure 8** Effect of GKAP  $\Delta R1$  mutant on the PTX-induced expression of Arc and Plk2 and on the Plk2-mediated removal of PSD-95. **(a)** Effect of GKAP WT and  $\Delta R1$  mutant overexpression on PTX-induced expression of endogenous Arc. Hippocampal neurons (21 DIV) were transfected with either  $\beta$ -Gal alone, WT, or  $\Delta R1$ . At 1 d post-transfection, neurons were treated with either DMSO (Control) or PTX (100  $\mu$ M), further incubated for 2 d, and examined for Arc (red) by immunofluorescent staining. **(b)** Quantification of PTX-induced Arc expression.  $n > 20$  per condition. \*\*\*  $P < 0.001$ . **(c)** Effect of GKAP WT and  $\Delta R1$  mutant overexpression on PTX-induced expression of endogenous Plk2. Hippocampal neurons (18 DIV) were transfected, treated with PTX as described in **(a)**, and examined for Plk2 (red) by immunofluorescent staining. **(d)** Quantification of PTX-induced Plk2 induction.  $n > 20$  per condition. \*\*\*  $P < 0.001$ . **(e)** Effect of GKAP turnover mutants on the Plk2-induced removal of synaptic PSD-95. Hippocampal neurons (18 DIV) were transfected with either Plk2 alone, Plk2 + WT, Plk2 +  $\Delta R1$ , or Plk2 + S54A and examined for their effect on endogenous PSD-95 at 2 d post-transfection. **(f,g)** Quantification of the Plk2-induced removal of PSD-95, measured by the PSD-95 cluster density **(f)** or intensity **(g)** in proximal dendrites. Scale bars, 20  $\mu$ m **(a,c)**, 5  $\mu$ m **(e)**.



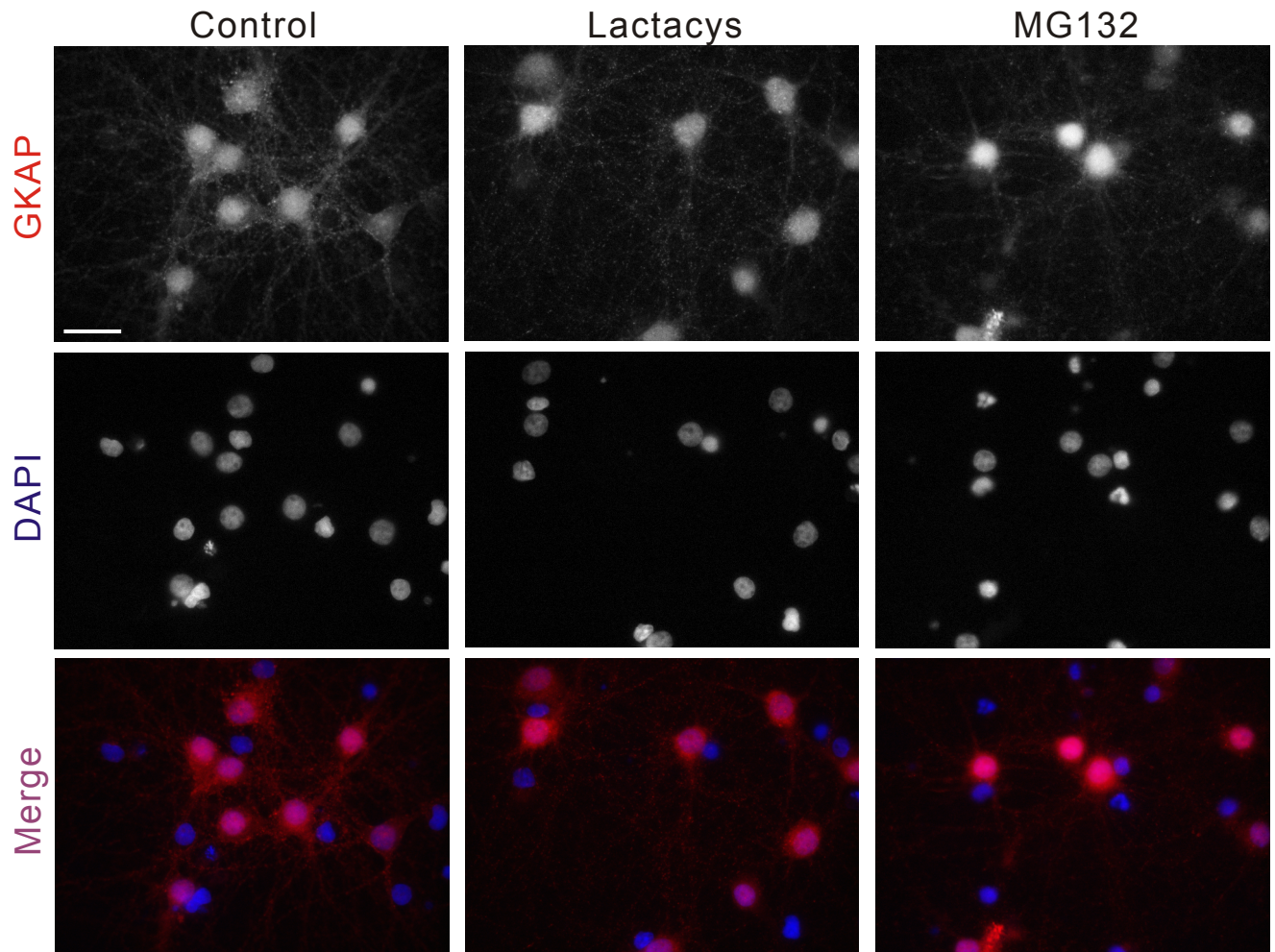
**Supplementary Figure 9** Schematic models for GKAP turnover at synapses. **(a)** Mechanism for GKAP degradation during elevated activity. ① Increased Ca<sup>2+</sup> influx through NMDA receptor activation leads to the activation of  $\alpha$ -CaMKII. ② Activated  $\alpha$ -CaMKII phosphorylates S54 and S201 in the N-terminal R region of GKAP, which uncouples GKAP from PSD-95. ③ S54 phosphorylation promotes poly-ubiquitination and removal of GKAP from synapses. ④ Poly-ubiquitinated GKAP is degraded by proteasomes presumably outside dendritic spines. **(b)** A model for GKAP recruitment to synapses. ① GKAP is transported to the base of dendritic spines by MyoVa-DLC motor complex that runs on actin cytoskeleton. ② Ca<sup>2+</sup> influx through VDCC leads to the preferential activation of actin-associated  $\beta$ -CaMKII. ③ Activated  $\beta$ -CaMKII phosphorylates S340 and S384 in the DLC-binding region of GKAP, which uncouples GKAP from DLC-MyoVa motor complex. ④ “Unloaded” GKAP integrates into PSDs.



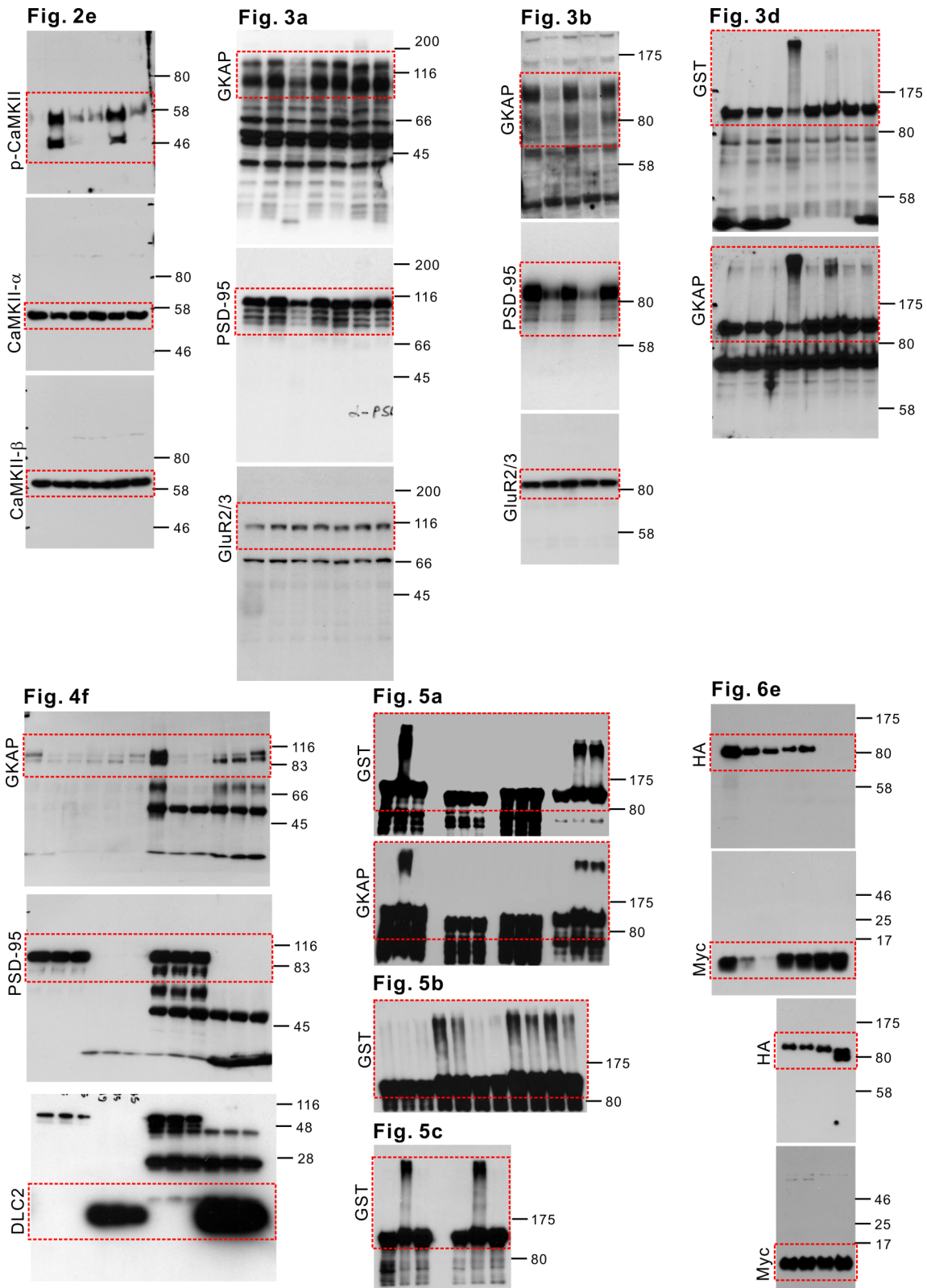
**Supplementary Figure 10** GKAP ( $\Delta$ R1) forms coclusters with PSD-95 regardless of  $\alpha$ -CaMKII activation. Effects of  $\alpha$ -CaMKII (T286D) on co-cluster formation between GKAP ( $\Delta$ R1) and PSD-95. HA-GKAP ( $\Delta$ R1) and Myc-PSD-95 were co-transfected in COS cells without (a1) or with  $\alpha$ -CaMKII (T286D) (a2). Cocluster formation is examined by double immunofluorescence staining (green, GKAP; red, PSD-95).



**Supplementary Figure 11** Activity-dependent changes of synaptic protein clusters. **(a)** Full image of GKAP and PSD-95 double immunofluorescence staining in hippocampal neurons (untreated control). Green and red arrows indicate GKAP- and PSD-95-dominant puncta, respectively. Note that GKAP shows more pronounced staining in the soma than PSD-95. **(b)** Activity-dependent changes of synaptophysin. Representative images are shown on the left and quantified data are shown on the right.  $n = 12$  per condition. Scale bars,  $20 \mu\text{m}$  **(a)**,  $5 \mu\text{m}$  **(b)**. **(c)** Cumulative distribution analysis of GKAP cluster intensities from control and Bic-treated neurons.  $n = 162$  from each condition.  $P < 0.0001$  (K-S test).



**Supplementary Figure 12.** DAPI staining of hippocampal neurons treated with DMSO (Control), Lactacystin (10  $\mu\text{M}$ ), or MG132 (50  $\mu\text{M}$ ) for 24 h. GKAP was counter-stained with anti-GKAP antibody and Cy3-conjugated secondary antibody (red). Note that all neurons showing GKAP clusters in dendrites show intact nuclei, indicating that proteasome inhibitors did not induce significant apoptosis in these neurons. Scale bar, 20  $\mu\text{m}$ .



**Supplementary Figure 13** Uncropped full-length blots for figures in the main text. Dashed rectangles (red) indicate the cropped regions shown in the main figures. Antibodies used are shown on the left and the relative positions of molecular weight markers are indicated on the right (kDa).